Investigation of the Soret effect in aqueous and non-aqueous mixtures by the thermal lens technique

Pavel Polyakov[1,*] and Simone Wiegand[1,†]

[1]Forschungszentrum Jülich GmbH,

IFF - Weiche Materie, D-52428 Jülich, Germany

(Dated: August 26, 2008)

1

Abstract

In the present work we investigate the thermal diffusion behavior of three different binary mixtures with a thermal lens (TL) setup. In the setup used in this study we avoid the addition of a dye for systems, such as aqueous mixtures, with a weak absorption band at a wavelength of 980 nm. In some aqueous systems with a complex phase behavior the addition of dye significantly affects the apparent measured thermal diffusion properties. The studied systems are dimethylsulfoxide (DMSO) in water, the ionic liquid 1-ethyl-3-methylimidazolium ethylsulfate (EMIES) in butanol and a non-ionic surfactant hexaethylene glycol monododecyl ether ($C_{12}E_6$) in water. The Soret coefficients of the selected systems cover a range of two orders of magnitude. For DMSO in water with a very low Soret coefficient of the order of $S_T \sim 10^{-3} K^{-1}$ we find for a low DMSO content ($c = 0.33$) a reasonable agreement with previous measurements, while the weak thermal lens signal for the DMSO-rich mixture ($c = 0.87$) leads to 20% too large Soret coefficients with an uncertainty of more than 30%. Secondly we studied a liquid salt 1-ethyl-3-methylimidazolium ethylsulfate (EMIES) in butanol with a roughly ten times higher Soret coefficient of $S_T \sim 10^{-2} K^{-1}$. For this system we performed additional measurements with another experimental technique, the classical thermal diffusion forced Rayleigh scattering (TDFRS), which requires the addition of a small amount of dye to increase the absorption. In the entire investigated concentration range the results obtained with the TL and classical TDFRS technique agree within the error bars. As a third system we studied a non-ionic surfactant hexaethylene glycol monododecyl ether ($C_{12}E_6$) in water with a Soret coefficient of the order of $S_T \sim 10^{-1} K^{-1}$. For this system we find good agreement with previous measurements. We conclude that the TL technique is a reliable method for systems with a strong optical contrast and fairly large Soret coefficient of the order of $S_T \sim 10^{-2} K^{-1}$.

PACS numbers:

I. INTRODUCTION

Thermal diffusion describes the migration of molecules in a temperature gradient. As a result of this process a concentration gradient builds up. In the steady state when the mass flux vanishes, the concentration gradient is given by

$$\nabla c = -S_{\mathrm{T}} c(1-c) \nabla T, \tag{1}$$

where $S_{\mathrm{T}} = D_{\mathrm{T}}/D$ is the Soret coefficient, D_{T} is the thermal diffusion coefficient, D is the translational diffusion coefficient, c is the weight fraction. A positive Soret coefficient of the component with the weight fraction c implies that this component moves to the cold region.

The main practical applications are separation processes[1,2] such as thermal field flow fractionation of polymers and colloids or isotope separation, characterization of geochemical processes[3,4] and combustion[5].

Even less than 20 years ago, different experimental techniques such as thermo gravitational columns, beam deflection, diffusion cells and thermal diffusion forced Rayleigh scattering (TDFRS) gave different results for simple organic mixture such as toluene/n-hexane[6–8]. The reason for the deviations are manifold, like technical imperfections and the presence of convection. Therefore, a benchmark test has been initiated, to measure thermal diffusion properties of simple organic mixtures by different experimental techniques[9].

The principle of the classical TDFRS method is as follows: a grating created by the interference of two laser beams is written into a sample. Except for the recently developed IR-TDFRS[10], a small amount of dye present in the sample converts the intensity grating into a temperature grating which in turn causes a concentration grating by thermal diffusion. Both gratings, temperature and concentration, contribute to a refractive index grating, which refracts a third laser beam. The time dependence of the diffracted signal intensity is analyzed and gives the diffusion coefficient D, the thermal diffusion coefficient D_T and the Soret coefficient S_T. In the benchmark test it was demonstrated that the classical TDFRS method gives reliable results for organic mixtures and also the data obtained for simple aqueous systems compare well with other experimental techniques[11–14]. However, recent studies on the surfactant hexaethylene glycol monododecyl ether ($C_{12}E_6$) in water with the classical TDFRS showed, that the small amount of dye added to create a temperature grating, leads to an unexpected second mode in the concentration part of the classical TDFRS signal[15,16].

The thermal lens (TL) technique is another powerful method which can be used to study the Soret effect in liquid mixtures, ferrofluids and micellar solutions[17–20]. The basic principle of the TL experiment is that a focused laser beam causes local heating in a sample, which leads in a mixture first to a thermal lens (local refractive index change due to temperature variations) and then to a Soret lens (local refractive index change due to concentration variations). In some of the experiments[20] a small amount of dye is added to achieve a sufficient heating by the laser beam others use a weak absorption band of water in the infrared[19]. First, Gordon et al.[21] observed the thermal lens effect in a liquid placed within the resonator of a helium-neon laser. Later, Giglio and Verdramini[22] noticed that the thermal lens in a binary mixture was noticeably larger than in pure components. The first careful theoretical analysis of the TL effect was done by Norman et al.[23] and Carter et al.[24]. The thermal lens method has been used to study the sign of the Soret coefficient of ferrofluids[17] and to measure S_T for ferrofluids[18] as well as for ionic surfactant systems[19] and Ludox particles in water[19]. The Soret coefficient for Ludox particles in water is only for small Debye lengths consistent with results from classical TDFRS, while for larger Debye lengths S_T determined by TL experiments is significantly larger than in the classical TDFRS[25]. The obtained Soret coefficient for maghemite nanograins coated with negatively charged citrate ions and dispersed in water (ferrofluids) agreed to some extent with measurements obtained by a transient grating technique (deviations are of the order of 20%)[18]. In contrast, Voit[26] measured 40% smaller Soret coefficient for benchmark n-dodecane/1,2,3,4 tetrahydronaphtalene mixture. This disagreement can be explained by convection, which results in better mixing, making the Soret coefficient smaller.

In many points the TDFRS and TL setups are comparable. Both techniques are optical methods, which rely on the refractive index contrast of the mixture, and, except for a few special cases[27], both methods are limited to binary mixtures. In the TDFRS experiments two lasers are needed with a coherence length of the order of a few centimeters to produce a holographic grating in the sample and to allow for heterodyne signal detection. Additionally, the wavelengths of the two lasers need to be so far apart that the sample absorbs the light at one wavelength, while the sample has to be transparent for the other wavelength. The use of two different wavelengths makes it also more difficult to change the wavelength of the writing beam. In the TL experiment the laser needs to have a stable Gaussian profile with a good stability. The grating vector q is well defined in the TDFRS experiment which enables

a detailed analysis of polydisperse systems[28]. In total the equipment requirements and costs are higher for TDFRS than for the TL. In general the equilibration times for the TL is 30-times higher than for TDFRS, which makes the TDFRS more suitable for very slow diffusing particles. The weakest point of the TL setup is its sensitivity to convection which can be a problem for slow diffusing systems and systems with a low optical contrast. In the first case convection often sets in before equilibrium is reached. In the latter case a thicker sample cell would be used to increase the contrast, which however leads to enhanced convective flow. Due to the small dimension in the TDFRS experiments convection, is usually not a problem. To check for the occurence of convection TDFRS experiments are often repeated at different powers of the writing beam and the coefficients are extrapolated to a power of zero. Nevertheless, for many systems with a good signal to noise ratio, the TL method is a compact and robust method to measure the thermal diffusion properties of liquid mixtures, polymer solutions and dispersions of small colloidal particles with a radius below 100 nm.

The goal of this paper is to validate the thermal lens technique as a method to measure thermal diffusion properties. The database for reliable Soret coefficients and thermal diffusion coefficients is still very small. As mentioned before the only benchmark test has been performed for organic mixtures[9]. The best studied aqueous system is ethanol/water[11–14], but the refractive index of ethanol ($n = 1.359$) is very close to that of water ($n = 1.333$), so that we expected that it would be difficult or impossible to measure this system with the thermal lens setup. Therefore, we chose dimethylsulfoxide (DMSO), which has a higher refractive index ($n = 1.479$) and it has also been measured before. During the experiments it turned out that the strength of the signal was not sufficient in the entire concentration range. We looked for a simple system with a larger Soret coefficient and chose the ionic liquid 1-ethyl-3-methylimidazolium ethylsulfate (EMIES). It was found that EMIES decomposes in the presence of water to form 1-ethyl-3-methylimidazolium hydrogen sulfate and ethanol under ambient conditions[29], so that we used instead of water butanol as solvent, which shows a sufficient absorption in the near infrared. To our best knowledge is the first time that a ionic liquid mixtures has been investigated. As a complex and interesting system we finally investigated the non-ionic surfactant system $C_{12}E_6$ in water, which also has been investigated before by classical TDFRS[16] and was one of our motivations to build this set-up and the IR-TDFRS[10,30]. For these three types of mixtures the Soret coefficient S_T differs by orders of magnitudes (10^{-3}, 10^{-2} and 10^{-1} K^{-1}, respectively). All three systems

show a sufficient absorption at $\lambda = 980$ nm, so that we do not need to add a dye in the TL experiment. The obtained results for DMSO/water and $C_{12}E_6$ in water were compared with recent measurements obtained with the classical TDFRS, which needs a small amount of dye to assure a sufficient absorption of the wavelength of the writing beam[31]. In the case of the ionic liquid we performed additional measurements with classical TDFRS, because for this system no literature data are available. The previous measurement for the non-ionic surfactant system with the classical TDFRS showed that the addition of the dye causes changes in the measured thermal diffusion behavior[16]. We compare the TL measurements with recent measurements using IR-TDFRS[30], which works also without dye if the system shows sufficient absorption at $\lambda = 980$ nm.

II. EXPERIMENT AND WORKING EQUATIONS

A. Sample Preparation.

Hexaethylene glycol monodecyl ether ($C_{12}E_6$; $\geq 98\%$) was ordered from Nikkol Chemicals (Tokyo). Butanol (99.5%), dimethylsulfoxide (DMSO; 99.7%) were purchased from Sigma-Aldrich and 1-ethyl-3-methylimidazolium ethylsulfate (EMIES; 99%) was ordered from Solvent Innovation GMBH. We took deionized water Milli-Q. All chemicals were used without further purification. The aqueous solutions of DMSO were prepared without dye. The EMIES/butanol mixtures for classical TDFRS contain a small amount (roughly 10^{-6} wt %) of the dye quinizarin (Aldrich). The amount of the dye corresponds to an optical density of 1 cm^{-1} at a wavelength $\lambda = 488$ nm, while in the TL experiments no dye was used. The aqueous solutions of the non-ionic surfactant $C_{12}E_6$ were investigated by the TL method with and without dye. In this case we used the water soluble dye basantol yellow. After the non-ionic surfactant $C_{12}E_6$ had been added to the water the solution was stirred at least for four hours at room temperature.

B. Refractive index increment measurements.

Refractive indices were determined using an Abbe refractometer. The refractive index increment $(\partial n / \partial c)_{p,T}$ at constant pressure and temperature was determined from the derivative of a second order polynomial fit of refractive index data. The temperature derivatives of

the refractive index $(\partial n/\partial T)_{p,c}$ at a constant pressure and concentration were determined in a temperature range $T \pm 3\,°C$ using a Michelson interferometer[32]. The refractive index increments for the binary mixture of DMSO/water and the surfactant solution of $C_{12}E_6$/water were taken from Ning et al.[16,31].

C. TDFRS experiment and data analysis

The classical TDFRS and the IR-TDFRS experiment are described elsewhere in detail[10,16]. An argon-ion laser (λ_w=488 nm) or infrared laser (λ_w=980 nm) are used for writing a grating. The laser beam is splitted into two writing beams of equal intensity by a beam splitter. An intensity grating is created in the sample by the interference of these two laser beams. In a classical TDFRS experiments a small amount of dye in the sample converts the intensity grating into a temperature grating. While in the IR-TDFRS the absorption at λ_w=980 nm is utilized to convert the light grating into a temperature grating, which in turn causes a concentration grating by the effect of thermal diffusion. Both gratings contribute to a combined refractive index grating, which is read out by diffraction of a third laser beam (λ_r=633 nm).

The heterodyne signal intensity $\zeta_{\text{het}}(t)$, normalized to the thermal signal, is related to the Soret coefficient as follows

$$\zeta_{\text{het}}(t) = 1 - A \left(1 - e^{-q^2 D t}\right) \tag{2}$$

with

$$A = \left(\frac{\partial n}{\partial T}\right)_{p,c}^{-1} \left(\frac{\partial n}{\partial c}\right)_{p,T} c\,(1-c)\,S_{\text{T}}$$

where q is the grating vector, D is the translational diffusion coefficient and A is the amplitude of the concentration signal.

To determine transport coefficients, Eq. 2 is fitted to the measured heterodyne signal taking into account the deficiencies of the Pockels cell by an iterative correction algorithm[16] and the two contrast factors $(\partial n/\partial c)_{p,T}$ and $(\partial n/\partial T)_{p,c}$, which are measured separately. Figure 1 shows a typical diffraction signal for the ionic liquid mixture EMIES/butanol. For all three concentrations we observe a negative concentration plateau indicating that the ionic liquids EMIES accumulates in the warm region.
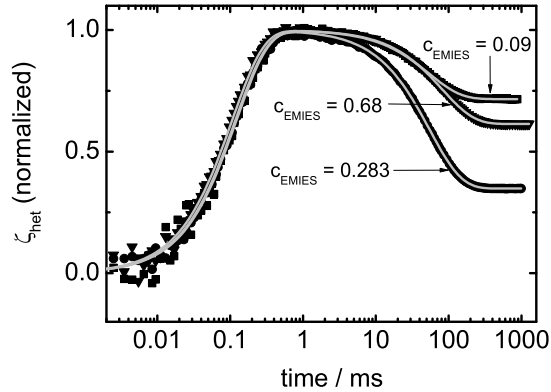
FIG. 1: Typical normalized classical TDFRS signals of EMIES/butanol mixtures in a cell with $l = 0.2$ mm for three different weight fractions c of the ionic liquid EMIES at 30°C. Solid symbols show the experimental results, lines are the fitted curves according to Eq. 2.

D. Thermal lens experiment and data analysis

1. Thermal lens effect

The principle of the TL method is described elsewhere in details[19,24]. The TL setup is sketched in Fig. 2. The mechanical shutter between the first and the second lens is used for "switching" the laser beam. The focused Gaussian laser beam illuminates a weakly absorbing sample, generating a temperature gradient within a characteristic time τ_{th}. Later a concentration gradient within a characteristic time $\tau_{\text{Soret}} >> \tau_{\text{th}}$ is induced by the Soret effect. The characteristic times τ_{th} and τ_{Soret} can be calculated using

$$\tau_{\text{th}} = \frac{\omega^2}{4D_{th}}; \qquad \tau_{\text{Soret}} = \frac{\omega^2}{4D}; \tag{3}$$

where ω is the beam size at the cell position, D_{th} and D are the thermal diffusivity and the translational diffusion coefficient, respectively. The thermal and Soret lenses are formed due to the dependence of the sample refractive index on temperature and concentration, respectively. The resulting time dependence of the beam center intensity can be used in order to estimate the thermal conductivity $\kappa = \rho c_p D_{th}$ and the Soret coefficient S_{T}. Here, ρ and c_p refer to the density and the heat capacity at constant pressure, respectively. In order to measure the intensity in the center of the beam, we place a detector with pinhole
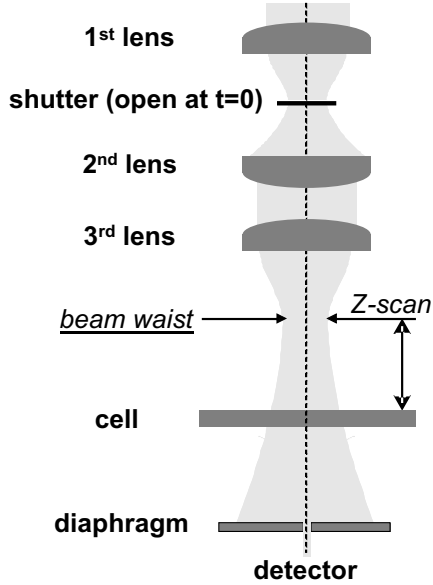
8

FIG. 2: Schematic drawing of the TL setup in an upright configuration.

at a large distance ($d_{sd} = 130$ cm) from the sample cell.

2. Working equations

In the following section we present the working equations to describe the TL effect. In a binary mixture the thermal lens is created in two steps. First the thermal lens is formed, which is characterized by the time constant τ_{th} and the strength of the thermal lens θ_{th}. Secondly the Soret lens or concentration lens is formed, which is described with an analog formalism. The relevant parameters are the characteristic time constant τ_{Soret} and the strength of the Soret lens θ_{Soret}.

The thermal lens is induced by a Gaussian beam with a power P and a wavelength λ in a sample with absorbtion coefficient b and thermal diffusivity D_{th}. The full expression for the position and time dependence of the beam center intensity response is given by

$$I(t) = I(0)(1 + f(\theta_{th}, \gamma, \tau_{th}, t));\tag{4}$$

$$\text{with} \quad f(\theta_{th}, \gamma, \tau_{th}, t) = A(\gamma, \tau_{th}, t)\theta_{th} + B(\gamma, \tau_{th}, t)\theta_{th}^2$$

The parameter θ_{th} characterizes the strength of the thermal lens in the sample and is given by

$$\theta_{th} = -\frac{0.52 P b l}{\kappa \lambda} \frac{\partial n}{\partial T},\tag{5}$$

9

where l is the cell thickness, κ is the thermal conductivity of the sample. The dimensionless parameter $\gamma = \triangle z \, z_R^{-1}$ is the distance from the cell to the beam waist with $\omega = \omega_0$ rescaled to the Rayleigh range z_R, which is the distance between the beam waist and the point with beam radius $\omega = \sqrt{2}\omega_0$. The coefficients A and B are equal to,

$$A(\gamma, \tau_{th}, t) = -\mathrm{atan}\left[\frac{2\gamma}{3 + \gamma^2 + (9 + \gamma^2)\tau_{th}/2t}\right] \tag{6}$$

$$B(\gamma, \tau_{th}, t) = \frac{A^2}{4} + \left(\frac{1}{4}ln\left[\frac{[(2 + \tau_{th}/t)(3 + \gamma^2) + 6\tau_{th}/t]^2 + 16\gamma^2}{(9 + \gamma^2)(2 + \tau_{th}/t)^2}\right]\right)^2 \tag{7}$$

In order to take into account the Soret effect the additional term

$$f(\theta_{Soret}, \gamma, \tau_{Soret}, t) = A(\gamma, \tau_{Soret}, t)\theta_{Soret} + B(\gamma, \tau_{Soret}, t)\theta_{Soret}^2 \tag{8}$$

needs to be added to Eq. 4. The Soret coefficient S_T for binary mixture with concentration c and the refractive index derivatives $(\partial n/\partial T)$,$(\partial n/\partial c)$ can be obtained from the ratio of the strength of the Soret lens θ_{Soret} and the strength of the thermal lens θ_{th} in the sample

$$S_T = -\frac{\theta_{Soret}}{\theta_{th}}\frac{\partial n/\partial T}{\partial n/\partial c}c^{-1}(1 - c)^{-1}; \tag{9}$$

There are two ways to analyze the experimental data. Typically we fixed the distance between the cell and the beam waist and recorded the time dependence of the intensity $I(t)$, which can be analyzed according to Eq. 4. Another way to analyze the data is by calculating the expression $(I(0) - I(t = \infty))/I(t = \infty)$ with the intial intensity $I(0)$ and the intensity at infinite times $I(t = \infty)$ at different positions. The final expression of this so-called z-scan method can also be derived from Eq. 4. Both appraoches can be found in the literature[18,19] and they should give the same results. Finally the thermal conductivity κ and the Soret coefficient S_T can be calculated according to Eq. 5 or 9, respectively.

3. Thermal lens setup

The schematic diagram of the experimental setup is shown in Fig. 2. In order to decrease convection effects our setup has been constructed with an upright optical axis. We have used an infrared laser ($\lambda = 980$nm) with a maximum output power of $P = 50$ mW. The laser was connected with the setup via a monomode fiber. We used a mechanical shutter between the first and the second lens for "switching" the laser beam. The third lens (focal length

100mm) focuses the parallel beam into the sample cell. For all positions along the optical path the cell is mounted perpendicular to the beam. In order to measure the intensity in the center of the beam we place a pinhole with a diameter of 4 mm in front of the photodiode, which was placed at a distance of $d_{sd} = 130$ cm from the sample cell.

The process of alignment consists of four steps. First, the xy-position as well as the angle of the laser beam were adjusted using a CCD camera (Coherent Lasercam HR), which records the laser profile. The pinhole was moved along the optical path, while the position of the beam center was monitored by the CCD camera at the same postion, where the photodiode is mounted during the measurement. Secondly, the position of the photodiode with the pinhole has to be adjusted using an infrared viewer. The third step is the optimization of the xy-position of each lens, which is done by analyzing the laser profile behind a pinhole, which is placed in the focus of the lens. The same procedure is repeated for each lens with the same pinhole as in the first step. The angle for each lens was adjusted by checking the back reflection on the same pinhole using the infrared viewer. Finally, the cell was slightly tilted to avoid back reflection in the laser diode.

In order to avoid vibrations of the setup during the experiment we mounted the shutter on a separate column and we avoided circulating water for temperature control of the cell. The cell was placed in the copper block, which was heated from both sides by two Peltier elements. The temperature was controlled with an uncertainty $\Delta T = \pm 0.01$ K (Peltron). At the maximum experimental temperature $T = 40°$C the temperature difference between the center and the edge was of the order of 0.05 K. All experiments were performed with a power of typically $P = 21 \pm 1$ mW. The distance between the cell and the beam waist was 3 - 4 mm.

4. *Calibration of the thermal lens set-up*

First, we show that we can reproduce the TL signal of pure water with our setup. Fig. 3 (curve (a)) shows a typical time dependence of the intensity in the center of the beam for pure water at room temperature. From this dependence the fractional change in the center beam intensity $(I(0) - I(\infty))/I(\infty)$ at a given distance from the cell to the beam waist can be calculated. The full coordinate dependence of this parameter at different powers for a cell with $l = 5$ mm as a function of the distance to the beam waist (called z-scan) is shown in
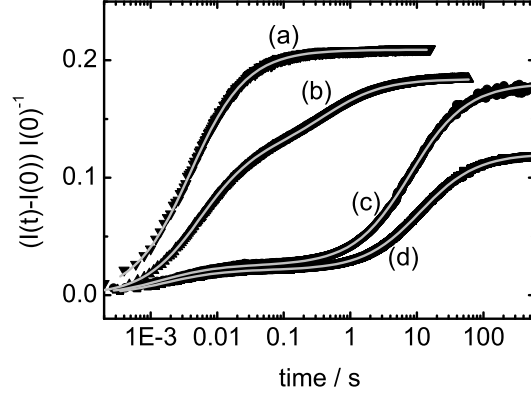
11

FIG. 3: Typical TL signals: (a) pure water at 22°C in a cell with $l = 5$ mm; (b) DMSO ($c = 0.33$wt%) in water ($c = 0.67$wt%) at 25°C in a cell with $l = 1$ mm; (c) $C_{12}E_6$($c = 0.1$wt%) in water ($c = 0.9$wt%) at 30°C cell 0.2mm; (d) $C_{12}E_6$ ($c = 0.05$wt%) in water ($c = 0.95$wt%) at 30°C in a cell with $l = 0.2$ mm. Solid symbols show the experimental results, lines correspond to the fit using Eq. 4 (pure TL effect in case (a)) or with taking into account additional term for describing the Soret effect (c.f. Sec. II D 2).
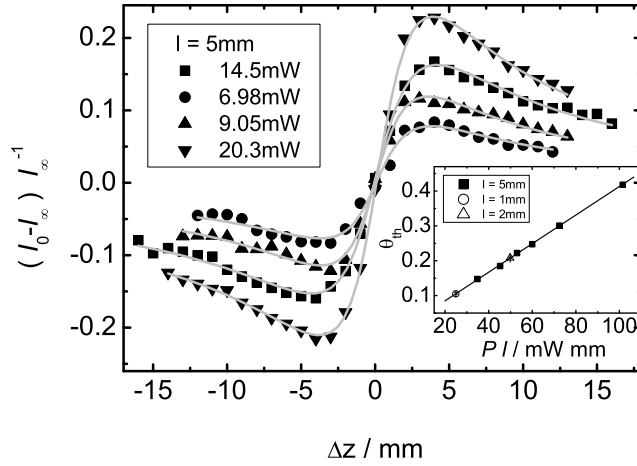

FIG. 4: Typical z-scan curves for pure water in cell with $l = 5$ mm at 22°C for different laser powers. These curves are fitted using Eq. 4 (c.f. Sec. II D 2). The inset shows the thermal lens number θ_{th} obtained from z-scan data at different laser powers P and cell thicknesses l as a function of the product Pl. Straight line is according to Eq. 5.

TABLE I: Characteristic convection times for different solvents calculated from convection velocity[19] in pure water in a cell with $l = 0.5$ mm at $P = 20$ mW for our experimental conditions using Eq.10, which is valid for low Grashof numbers ($Gr \ll 1$)).

solvent	temperature difference ΔT / K	cell thickness / mm	Gr number	$\tau_{\text{convection}}$ s
water	0.49	0.2	$7.6 \ 10^{-3}$	141
		1	$9.5 \ 10^{-1}$	>6
butanol	0.26	0.2	$2.1 \ 10^{-3}$	164
		1	$2.6 \ 10^{-1}$	>7
DMSO	0.14	0.2	$2.6 \ 10^{-3}$	218
		1	$3.2 \ 10^{-1}$	>9

Fig. 4. The solid lines correspond to the fit according to Eq. 4 and 5. The inset shows the values of θ_{th} calculated from the z-scan data at different powers (P) and cell thicknesses (l) versus Pl. The data are well described with $b = 0.5$ cm^{-1} (Ref. 19), $\partial n/\partial T = -0.9378 \ 10^{-4}$ K^{-1} (Ref. 14) and $\lambda_{laser} = 980$ nm according to Eq. 5. The heat conductivity was found to be equal 0.6098 Wm^{-1}K^{-1}, which is quite close to the tabulated value 0.603 Wm^{-1}K^{-1} in Ref. 33.

For pure butanol at 30°C the heat conductivity was determined from the time dependence of the central beam intensity. The obtained value 0.1542 Wm^{-1}K^{-1} ($l = 1$ mm, $P = 20.05$ mW, $\theta_{\text{th}} = 0.1784$, $b = 0.066$ cm^{-1} and $\partial n/\partial T = -3.92 10^{-4}$ K^{-1}) is also in good agreement with the reference value 0.153 Wm^{-1}K^{-1} in Ref. 33.

5. *Convection effects in the thermal lens experiment*

Generally speaking, the non-zero extinction coefficient of our sample and the finite thickness of the cell lead to a temperature inhomogeneity in the direction parallel to the laser beam. The behavior of the components with different densities becomes sensitive to gravity, which is commonly known as convection. In order to avoid convection, the characteristic equilibration time should be smaller than the characteristic convection time ($\tau_{convection}$).

13

The convection time can be estimated through the ratio of the beam size at the cell position ($\omega \approx 54$ μm for a typical $\tau_{th} \approx 5$ ms for a cell with 1 mm with water, placed 4 mm before the beam waist; (c.f. Eq. 3) to the convection velocity $U_{convection}$. Rusconi et al.[19] proposed two expressions for scaling the convection velocity (c.f. Eq. 10 and 11).

$$U_{convection} \sim g\alpha l^2 \triangle T \nu^{-1}; \qquad Gr \ll 1; \tag{10}$$

$$U_{convection} \sim (g\alpha \nu l \triangle T)^{0.5}; \qquad Gr \gg 1, \tag{11}$$

where α is the thermal expansion coefficient, ν is the kinematic viscosity, g is gravitational acceleration and $\triangle T$ is the characteristic amplitude of the temperature inhomogeneity. The Grashof number Gr is defined as

$$Gr = g\alpha \triangle T l^3 \nu^{-2}. \tag{12}$$

Eq. 10 is only valid for low Grashof numbers ($Gr \ll 1$), while for large Grashof numbers (($Gr \gg 1$)) Eq. 11 needs to be used.

Rusconi et al.[19] calculated the convection velocity profiles in a cell with $l = 0.5$ mm and for a laser power of $P = 20$ mW using the Navier-Stokes equations. The maximum value in the center of the cell was found to be $U_{convection} \approx 2.4 \ 10^{-6}$ m s^{-1}. Scaling this value according to Eq. 10 with the cell thicknesses allows to calculate convection times for different cell thicknesses and different solvents. The obtained values are presented in Table I. The characteristic temperature difference ($\triangle T$) between the sample temperature at the center of the beam and the average sample temperature were calculated according to the criteria $\triangle T \approx 0.3 P b l \kappa^{-1}$, proposed by Gordon et al.[21]. The corresponding values are also presented in Table I.

III.   RESULTS AND DISCUSSION

A.   Nonionic surfactant $C_{12}E_6$ in water

Fig. 3 (curves (c) and (d)) shows typical TL signals obtained in a cell with $l = 0.2$ mm of $C_{12}E_6$ ($c = 0.1$wt%) and of $C_{12}E_6$ ($c = 0.05$wt%) in water at 30°C. In the entire range the fit shows no systematic deviations and the obtained values of the Soret coefficient at different
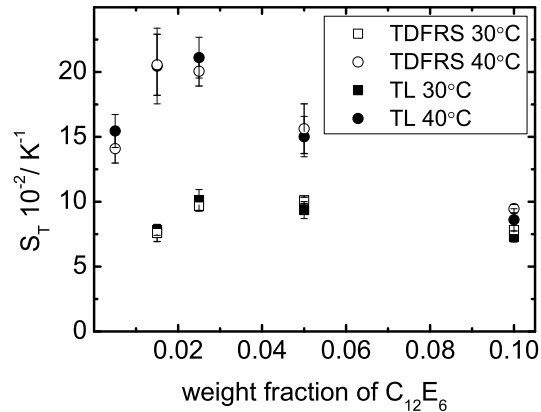
14

FIG. 5: Soret coefficient of $C_{12}E_6$ aqueous solutions at 30 and 40°C as a function of surfactant concentration. Open symbols are IR-TDFRS data[30], solid symbols refer to data from TL.

concentrations ($c = 0.005, 0.015, 0.025, 0.05$ and 0.1 wt%) and temperatures ($T = 30$ and 40°C) agree within the error bars with the Soret coefficients recently obtained by Ning et al. with the IR-TDFRS[30] (c.f. Fig. 5). The maximal deviation between IR-TDFRS and TL data is of the order of 14%, but no systematic trend could be observed. The characteristic plateaus at large times (c.f. Fig 3) indicate that convection effects are negligible, despite that the typical equilibration times of $\sim 100 - 200$ s are of the order of the characteristic convection time of ~ 140 s (c.f. Table I).

Figure 6 shows the Soret coefficient for $C_{12}E_6$ ($c = 0.025$ wt%) in water for different dye contents (basantol yellow) at 40°C. The influence of the dye is found to be crucial. Increasing the optical density from 0 to 2 cm^{-1} (typical condition for classical TDFRS measurements) makes S_T 35 % smaller. According to our previous studies[16,30] the addition of basantol yellow shifts the two-phase boundary towards higher temperatures. This is the main reason that the Soret coefficient becomes smaller with increasing dye content. At the same time we did not observe a second mode in TL nor in the IR-TDFRS experiment. Such a second mode hat been observed previously with the classical TDFRS[16]. The reason for the second mode in the classical TDFRS is probably some kind of feedback mechanism, which leads to an inhomogenous dye distribution in the sample[30].
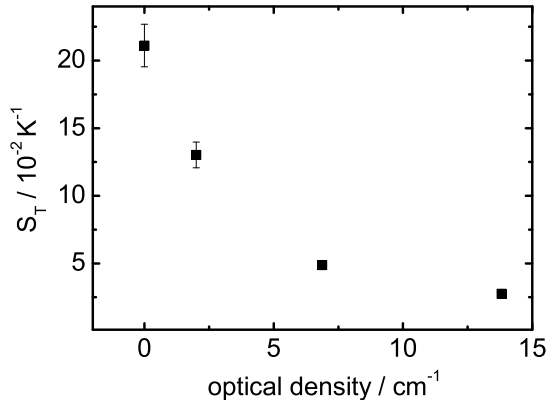
FIG. 6: Soret coefficient of $C_{12}E_6$ ($c = 0.025$wt%, $T = 40°C$) in water measured with the TL method in a cell with $l = 0.2$ mm as a function of the dye optical density.

B. DMSO in water

The Soret coefficient for DMSO/water is roughly two orders of magnitude smaller than for $C_{12}E_6$/water mixtures. In the case of an extremely weak thermodiffusion effect, for example close to a concentration, where D_T changes sign, one can expect that the Soret lens will be very weak and difficult to observe. Also thermal fluctuations and other sources of noise such as the stability of the laser will become important. Generally speaking, the sensitivity of the TL setup is associated with the amplitude A. If one compares both analysis equations Eq. 2 and 9 for TDFRS and TL, respectively, both methods are quite similar. The amplitude A in TDFRS is equivalent to the ratio of θ_{Soret} to θ_{th} in the TL method.

In order to have strong signal we chose two DMSO/water concentrations ($c = 0.33$ and 0.87) for which the amplitudes of the TDFRS signal are maximal (0.47 and 0.12, respectively). At the low DMSO content, DMSO moves to the cold side, while at higher DMSO content DMSO moves to the warm side. The typical TL signal for a mixture with a water mass fraction of 0.67 in a 1 mm cell is shown in Fig.3. The typical equilibration time for a 1 mm cell is of the order of the convection time (c.f. Table I).

The measured Soret coefficient in the water-rich region is $S_T = (2.5 \pm 0.4) \, 10^{-3}$ K^{-1} for a 0.2 mm cell and $S_T = (2.69 \pm 0.35) \, 10^{-3}$ K^{-1} for a 1 mm cell are in good agreement with the classical TDFRS data with $S_T = (2.7 \pm 0.04) 10^{-3}$ K^{-1}. The typical relative uncertainties of the TDFRS data are in the 2-3% range, while the TL data show 5 times higher noise.

16

In the DMSO-rich region it was not possible to measure reliable values in the 1 mm cell. The obtained Soret coefficient $S_T = -(3.85 \pm 1.3)\ 10^{-3}\mathrm{K}^{-1}$ is 18% larger than the value of $S_T = (3.23 \pm 0.06)\ 10^{-3}\mathrm{K}^{-1}$ obtained in the classical TDFRS. The uncertainty of the TL measurments exceeds 30%, while the uncertainty of the classical TDFRS measurements is of the order of 2%. In order to minimize convection effects we also performed measurements in the cell with $l = 0.2$ mm. In the thin cell, however, the concentration plateau was often not clearly seen and reproducible measurements were not possible. Under these conditions the Soret lens is too weak. Compared to measurements in the water-rich region the amplitude is 4 times smaller. The relative change in concentration $(\delta c/c)$ due to the temperature gradient was found to be $(\delta c/c) \approx 8 \cdot 10^{-5}$, which is one order of magnitude smaller than the corresponding value of $(\delta c/c) \approx 7 \cdot 10^{-4}$ in the water-rich region.

With the DMSO/water system we reach the limits of our thermal lens experiment. The typical noise level $\delta I/I$ in the TL experiment is of the order of 1% leading to an uncertainty in the order of 10 % to the concentration signal. This uncertainty of course influences the stability of the weak Soret lens. With our experimental equipment it was not possible to reduce the main reasons for noise such as vibrations, fluctuations in the intensity and temperature fluctuations further. Under our experimental conditions the signal needs to be at least comparable with one in the water-rich region with weaker noise and stronger Soret lens. Another possibility would be to increase the number repetitions in the TL experiment in order to reduce the error of the mean further. Here we need to keep in mind that an averaging of 2000-4000 measurements is unrealistic due to the roughly 100 times longer equilibration times in the TL experiment as compared to the TDFRS experiment.

C. Ionic liquid EMIES in butanol

The thermal diffusion behavior of EMIES/butanol mixtures was investigated in two different cells with $l = 0.2$ mm and $l = 1$ mm. Fig. 7 shows the typical TL signal for the mixture EMIES/ butanol ($l = 1$ mm). The characteristic equilibration time of $\sim 10 - 15$ s is again of the order of the convection time (c.f. Table I). The fitted function decribes the data well and the residuals are statistically distributed. The obtained Soret coefficients for different cells of varying thickness ($l = 0.2$ and 1 mm) for different EMIES concentrations ($c = 0.09, 0.283, 0.515$ and 0.68) at $T = 30°C$ agree within the error bars with the classical
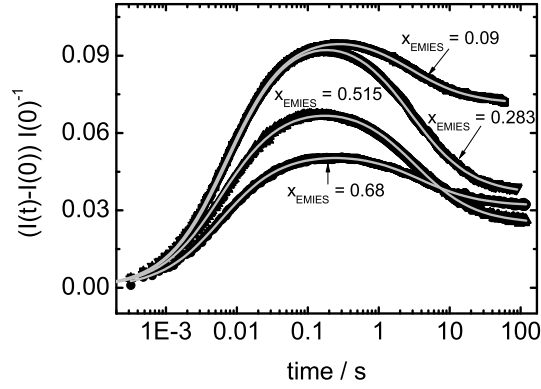
FIG. 7: Typical TL signals (cell 1mm) for solutions of EMIES in butanol at 30°C. Solid symbols show the experimental results, lines are the fitting curves according to Eq. 4 (pure TL effect) with taking into account the additional term that describes the Soret effect (c.f. Sec. II D 2).
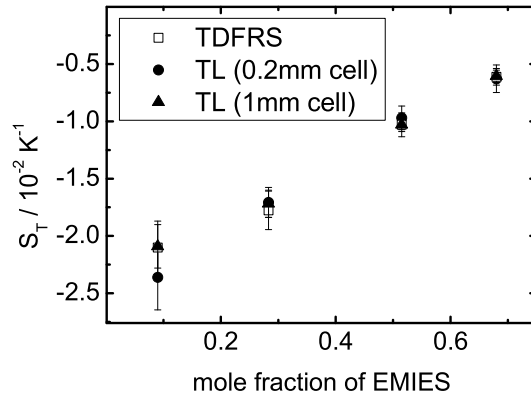

FIG. 8: Soret coefficient of EMIES in butanol at 30°C as a function of concentration. Open symbols are classical TDFRS data, solid symbols refer to TL data 0.2 mm and 1 mm cells.

TDFRS data. For the lowest salt concentration the maximum deviation found was 19%, but typically the values agree within 3-7%. The Soret coefficient is of the order of 10^{-2} K^{-1}, which is less than the characteristic value $(10^{-1}K^{-1})$ for $C_{12}E_6$/water and larger than $10^{-3}K^{-1}$ for DMSO/water mixtures. For the smallest value of S_T at the mass fraction of 0.68, the relative change in concentration due to the Soret effect $(\delta c/c) \approx 3.4 \cdot 10^{-4}$ is still larger than in case of solution of water in DMSO $((\delta c/c) \approx 8 \cdot 10^{-5})$.

18

IV. CONCLUSION

In the present work we compared the Thermal Diffusion Forced Rayleigh Scattering (TDFRS) technique with the Thermal Lens (TL) method. We investigated three different systems with Soret coeffcients between $S_T \sim 10^{-3} - 10^{-1} \text{K}^{-1}$. For the systems with the larger Soret coefficients we found good agreement between the two methods. For low Soret coefficients of the order of $S_T \sim 10^{-3} \text{K}^{-1}$, the TL method reaches its limits. In the case of a low Soret coefficient and a low optical contrast reliable measurements are not possible. Typically slow diffusing molecules such as polymers and colloids have fairly large Soret coefficient of the order of $S_T \sim 10^{-1} \text{K}^{-1}$, so that they are in principle good systems to be investigated by TL. The other limit of the TL experiment is that the characteristic equilibration time should be smaller than the characteristic convection time. Therefore the investigation of large colloids in the micron scale will be impossible.

A big advantage of the TL method is that it is fairly fast and the experimental setup is much cheaper compared to the TDFRS setups. It is also fairly easy to change the wavelength, so that the addition of dye can be avoided by using the natural absorption of the molecules. An important requirement on the laser source is an excellent Gaussian profile and laser stability, but the coherence length can be very short. If one plans future benchmark tests which should also include the thermal lens method, the systems have to be selected carefully so that the signal to noise ratio is also large enough to do precise TL experiments. According to our experiments ionic liquids such as EMIES in butanol seems to be a good candidate. The Soret coefficient is one order of magnitude larger than that for ordinary molecular sytems, which results in a sufficient signal to noise ratio in the TL experiment, while diffusion is still fast enough so that it is also accessible for other experimental techniques such as thermogravitational columns.

V. ACKNOWLEDGMENTS

1684).

* p.polyakov@fz-juelich.de; http://www.fz-juelich.de/iff/personen/P.Polyakov/

† s.wiegand@fz-juelich.de; http://www.fz-juelich.de/iff/personen/S.Wiegand/

[1] M. E. Schimpf and J. C. Giddings, *Macromolecules*, 1987, **20**(7), 1561–1563.

[2] K. Clusius and G. Dickel, *Naturwissenschaften*, 1939, **27**, 148–149.

[3] H. C. Helgeson, *Pure & Appl. Chem.*, 1885, **57**, 31–44.

[4] P. Costeseque, D. Fargue, and P. Jamet in *Thermal nonequilibrium phenomena in fluid mixtures*, ed. W. Köhler and S. Wiegand, Lecture Notes in Physics; Springer, Berlin, 2000; pp. 389–427.

[5] D. E. Rosner, R. S. Israel, and B. La Mantia, *Combustion and Flame*, 2000, **123**, 547–560.

[6] O. Ecenarro, J. A. Madariaga, J. Navarro, C. M. Santamaria, J. A. Carrion, and J. M. Saviron, *J.Phys.:Condens. Matter*, 1990, **2**(9), 2289–2296.

[7] W. Köhler and B. Müller, *J. Chem. Phys.*, 1995, **103**(10), 4367–4370.

[8] W. B. Li, P. N. Segre, R. W. Gammon, J. V. Sengers, and M. Lamvik, *J. Chem. Phys.*, 1994, **101**(6), 5058–5069.

[9] J. K. Platten, M. M. Bou-Ali, and J. F. Dutrieux, *Philos. Mag.*, 2003, **83**(17-18), 2001–2010.

[10] S. Wiegand, H. Ning, and H. Kriegs, *J. Phys. Chem. B*, 2007, **111**, 14169–14174.

[11] P. Kolodner, H. Williams, and C. Moe, *Journal of Chemical Physics*, 1988, **88**(10), 6512–6524.

[12] K. J. Zhang, M. E. Briggs, R. W. Gammon, and J. V. Sengers, *J. Chem. Phys.*, 1996, **104**(17), 6881–6892.

[13] J. F. Dutrieux, J. K. Platten, G. Chavepeyer, and M. M. Bou-Ali, *J. Phys. Chem. B*, 2002, **106**(23), 6104–6114.

[14] R. Kita, S. Wiegand, and J. Luettmer Strathmann, *J. Chem. Phys.*, 2004, **121**(8), 3874–3885.

[15] H. Ning, R. Kita, and S. Wiegand, *Progr. Colloid Polym. Sci.*, 2006, **133**, 111–115.

[16] H. Ning, R. Kita, H. Kriegs, J. Luettmer-Strathmann, and S. Wiegand, *J. Phys. Chem. B*, 2006, **110**, 10746–10756.

[17] S. Alves, G. Demouchy, A. Bee, D. Talbot, A. Bourdon, and A. M. F. Neto, *Philos. Mag.*, 2003, **83**(17-18), 2059–2066.

[18] S. Alves, A. Bourdon, and A. M. F. Neto, *Journal of the Optical Society of America B-Optical Physics*, 2003, **20**(4), 713–718.

19 R. Rusconi, L. Isa, and R. Piazza, *J. Opt. Soc. Am. B*, 2004, **21**(3), 605–616.

20 M. P. Santos, S. L. Gomez, B. E., and N. A. M. F., *Phys. Rev. E.*, 2008, **77**, 011403.

21 R. Gordon, R. Leite, R. Moore, S. Porto, and J. Whinnery, *J. Appl. Phys.*, 1965, **36**, 3.

22 M. Giglio and Vendrami.A, *Applied Physics Letters*, 1974, **25**(10), 555–557.

23 S. Norman and N. Dovichi, *J. Appl. Phys.*, 1989, **67**, 1170.

24 A. Carter and J. Harris, *J. Appl. Opt.*, 1984, **23**, 476.

25 H. Ning, J. K. G. Dhont, and S. Wiegand, *Langmuir*, 2008, **24**, 2426–2432.

26 A. Voit *Untersuchung von Transportprozessen in binären Flüssigkeiten mit Hilfe thermischer Linsen* Diplom, University Bayreuth, 2003.

27 B.-J. de Gans, R. Kita, S. Wiegand, and J. Luettmer Strathmann, *Phys. Rev. Lett.*, 2003, **91**, 245501.

28 W. Köhler and R. Schäfer in *New Developments in Polymer Analytics Ii*, ed. M. Schmidt, Vol. 151 of *Advances in Polymer Science;* Springer, Berlin, 2000; pp. 1–59.

29 L. E. Ficke, H. Rodrigez, and J. Brennecke, *J. Chem. Eng. Data*, 2008.

30 H. Ning, S. Datta, T. Sottmann, and S. Wiegand, *J. Phys. Chem. B*, 2008.

31 H. Ning and S. Wiegand, *J. Chem. Phys.*, 2006, **125**, 221102.

32 A. Becker, W. Köhler, and B. Müller, *Ber. Bunsen-Ges-Phys. Chem.*, 1995, **99**(4), 600–608.

33 C. Yaws, *Chemical Properties Handbook*, McGraw Hill, New York, 1999.